Multiple Nuclear Polarization States in a Double Quantum Dot

J. Danon, I. T. Vink, F. H. L. Koppens, K. C. Nowack, L. M. K. Vandersypen, and Yu. V. Nazarov
Kavli Institute of NanoScience, Delft University of Technology, 2628 CJ Delft, The Netherlands
(Received 16 February 2009; published 24 July 2009)

We observe multiple stable states of nuclear polarization and nuclear self-tuning over a large range of fields in a double quantum dot under conditions of electron spin resonance. The observations can be understood within an elaborated theoretical rate equation model for the polarization in each of the dots, in the limit of strong driving. This model also captures unusual features of the data, such as fast switching and a ''wrong'' sign of polarization. The results reported enable applications of this polarization effect, including accurate manipulation and control of nuclear fields.

DOI: 10.1103/PhysRevLett.103.046601 PACS numbers: 72.25.Pn, 73.23.−b, 73.63.Kv

Great experimental progress in the last decade enabled the confinement, initialization, and readout of single spins in quantum dots [1]. Controlled coherent single-spin rotations—a key ingredient for quantum manipulation—were demonstrated recently using the electron spin resonance (ESR) [2–6]. The weak hyperfine coupling of the electron spin to the nuclear spins in the host material appeared to be of great importance in this field. It was identified as the main source of qubit decoherence and provides a significant hybridization of the spin states [7,8]. This has stimulated intensive theoretical and experimental research focusing on nuclear spin dynamics in quantum dots [9–14].

Overhauser pointed out already in the 1950s [15] that ESR may provide the buildup of significant nuclear spin polarization. Indeed, most ESR experiments on quantum dots, aimed at demonstrating electron spin rotations, also clearly demonstrated dynamical nuclear spin polarization (DNSP) [2–5].

For ESR driving of a single spin in an almost isolated quantum dot, or an ensemble of such dots, the scenario is similar to that of the usual Overhauser effect: The direction of DNSP is parallel to the spin of the excited electrons [15,16]. Recent ESR experiments on self-assembled quantum dots have confirmed this picture [5], and a similar reasoning holds for spin experiments with optically pumped dots [17]. In some cases, a bistability has been observed: Under the same conditions, the nuclear spins in the dot can be either polarized or unpolarized [11].

However, several issues can complicate the situation. In recent ESR experiments in double quantum dots [2–4] (i) electrons participate in *transport* during ESR driving, and (ii) there can be different nuclear spin dynamics in the two dots. Furthermore, a driving magnetic field is in practice accompanied by an electric field which modulates the electron-nuclear spin coupling at the resonance frequency [4]. All this makes a straightforward extension of existing models [16] impossible and promises richer and more interesting physics, which we indeed reveal.

In this Letter, we report a study of ESR in a double quantum dot focusing on DNSP. We have observed multiple stable states of nuclear polarization (up to four states), not seen in single-dot experiments, nuclear self-tuning to the ESR condition over a large range of magnetic fields ($\gtrsim$100 mT), and a sign of DNSP opposite to that following from the Overhauser argument. We identify the most probable mechanism governing DNSP and present a theoretical model explaining our findings. The results reported enable applications of this self-tuning effect, including accurate manipulation and control of the nuclear polarization [18] and use of this for improving the electron spin coherence time, possibly by orders of magnitude.

The double quantum dot system is electrostatically defined in a two-dimensional electron gas, located 90 nm below the surface of a GaAs/AlGaAs heterostructure, by applying negative voltages to metal surface gates. The dots are tuned to the Pauli spin blockade regime [19], where the transport sequence of charge states is $(1, 1) \rightarrow (0, 2) \rightarrow (0, 1) \rightarrow (1, 1)$, (n, m) denoting the charge state with $n(m)$ excess electrons in the left(right) dot. The current through the double dot depends on the spin orientation of the electrons in the (1,1) state since the only accessible (0,2) state is a spin singlet (Fig. 1).

Magnetic spin resonance is achieved by sending an alternating current through a coplanar stripline (CPS) which lies on top of the surface gates, separated by a thin dielectric layer. This current produces a small oscillating magnetic field $B_1 \simeq 1$ mT perpendicular to the external magnetic field $B_0 \simeq 100$ mT. The experimental data are obtained with the same device and in the same measurement run as the data presented in Ref. [2]. The difference is that the device is tuned to a higher interdot tunnel coupling and coupling to the right lead.

When we apply a continuous wave RF current with fixed frequency ω to the CPS and sweep the external magnetic field B_0 passing the resonance condition $B_0 = B_{\mathrm{res}} \equiv \hbar\omega/g\mu_B$, we make a remarkable observation. One would expect that the resonance manifests itself as a peak in the current [2]. Indeed, if the external field is swept from low to high values, the current jumps up upon achieving the resonance condition. Unexpectedly, this resonant response extends over a wide range of magnetic fields, that exceeds B_{res} by a factor of 2 [see Fig. 2(a) upper panel]. If the field

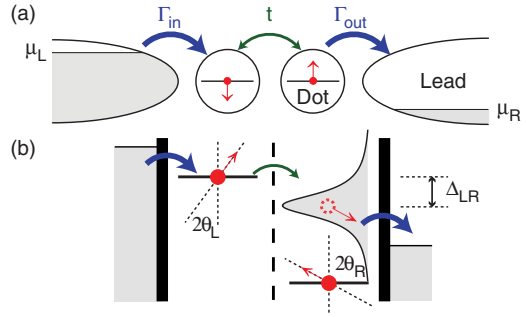

FIG. 1 (color online). Double dot setup. (a) The double quantum dot is coupled to two leads. Because of a voltage bias, electrons can only run from the left to the right lead. (b) Energy diagram. The four possible (1,1) states differ in spin projections on the quantization axes (red arrows). Under ESR conditions the axes can be different in the two dots and do not coincide with the direction of the external magnetic field. These states are coherently coupled (green arrow) to the (0,2) singlet that decays quickly (broadened line), leaving the system in (0,1).

is swept in opposite direction [Fig. 2(a) lower panel], the current remains low till B_0 is several mT above $B_{\rm res}$. This indicates a strong hysteresis for $B_0 > B_{\rm res}$, whereas the hysteresis below $B_{\rm res}$ is much less pronounced.

Another unexpected observation is made at fixed $B_0 \approx B_{\rm res}$. Instead of a single value of the current corresponding to the maximum value of the ESR satellite peak, we observe clearly distinguishable *multiple* stable values of the current. Switching between these values gives rise to a random telegraph signal (RTS) with time scales ranging from seconds to minutes. Typical time-resolved measurements of the RTS are presented in Fig. 2(b) for three different values of the energy level detuning Δ_{LR} (Fig. 1).

We associate both the hysteresis and RTS with DNSP induced by the nonequilibrium electron spin dynamics under conditions of ESR and transport in the dots. Nuclear polarization is known to provide an effective magnetic field B_N acting on the electron spin [15]. Where high current is observed in the hysteresis region, this extra field is such that the total field $B_0 + B_N \approx B_{\rm res}$, i.e., the nuclear field "tunes" the system to the resonance condition [16]. Low current indicates that $B_0 + B_N$ significantly deviates from $B_{\rm res}$: The nuclei are unpolarized. Both polarized and unpolarized states are stable in the interval of hysteresis. Fluctuations of any kind could provide spontaneous switching between stable states, leading to the RTS.

A number of experimental details does not fit into this simple picture. First, there are *multiple* values of the current observed, three are clearly visible in Fig. 2(b) (labeled A–C). This implies multiple stable states of nuclear polarization with a total field close to $B_{\rm res}$. Actually, we think that the RTS traces provide evidence for the existence of a fourth state. There is a number of current dips observed (labeled D) too big to be statistical fluctuations. We interpret those dips as signatures of a fourth state that decays on the scale of a second, i.e., different from state A, which decays on a larger time scale. Second, switching between the different current levels is rather fast. The nuclear spin dynamics are known to be slow, with a typical relaxation time $\tau_n \sim 15$ s [7,12,13]. If the current is a direct measure of the nuclear polarization, then why is the duration of the switching events so short? A third point is the *sign* of the polarization. Usually, in ESR experiments the dominating mechanism of DNSP is described by the Overhauser effect: The ESR excitation drives the electron spin(s) out of equilibrium, and hyperfine-induced electron-nuclear spin exchange is one of the mechanisms contributing to electron spin relaxation. As reasoned by Overhauser, on grounds of spin conservation, the direction of nuclear polarization should be parallel to the spin of excited electrons, whatever its orientation is with respect to the magnetic field applied. This is the case for most DNSP experiments, e.g., [2,5,11]. Given the negative g factor and positive hyperfine coupling in GaAs [20], this would give a B_N *parallel* to B_0 [16]. In

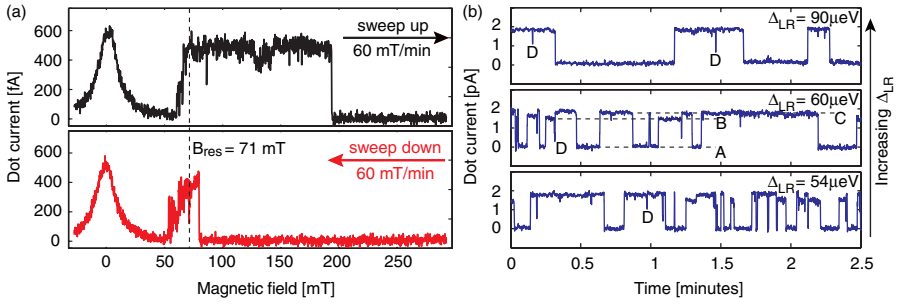

FIG. 2 (color online). (a) Magnetic field sweeps for ω fixed at 350 MHz. Upper panel: Magnetic field sweep from low to high values resulting in an ESR peak width exceeding 100 mT. Lower panel: Sweep in the opposite direction, showing a much narrower ESR peak [23]. The nominal resonance condition $B_{\rm res} = \hbar\omega/g\mu_B$ is met at $B_0 \approx 71$ mT for $\omega = 350$ MHz and $g = 0.35$ [2] (see dashed line). Note that in both traces the nuclear bath is unpolarized at the onset of electron spin resonance [22]. (b) Multiple values of the current through the double dot approximately at resonance. The current switches between at least three stable values on a time scale of seconds to minutes. The three panels correspond to three different values of the energy level detuning Δ_{LR} (increasing from the bottom to the upper panel). The values given for Δ_{LR} may have a constant offset, as photon assisted tunneling processes broaden the interdot transition which makes it difficult to separate resonant and inelastic transport. In both (a) and (b) the lowest value of current was subtracted as offset. The data in (b) were taken for a larger $\Gamma_{\rm in}$ and $\Gamma_{\rm out}$ than the data in (a).

our experiment, its direction is clearly *opposite*, as high current is seen for $B_0 > B_{\rm res}$. All three points are captured by the theory given below.

The electron spin $\hat{\mathbf{S}}$ and nuclear spins $\hat{\mathbf{I}}_k$ in each dot are coupled by hyperfine interaction [20] $\hat{H}_{\rm hf} = \frac{1}{2}\sum_k A_k\{2\hat{S}^z\hat{I}_k^z + \hat{S}^+\hat{I}_k^- + \hat{S}^-\hat{I}_k^+\}$, where the sum runs over $N \sim 10^6$ nuclei. The energy A_k is proportional to the probability to find the electron at the position of nucleus k, $A_k \simeq 10^{-10}$ eV. With an external field applied in the z direction, the "flip-flop" terms $\hat{S}^{\pm}\hat{I}_k^{\mp}$ provide spin exchange between the electrons and nuclei. Owing to energy conservation, these transitions must be second-order processes involving a mechanism supplying or absorbing the excess Zeeman energy. Conventionally, the spin exchange is due to the time-independent hyperfine coupling A_k. However, as recently has been pointed out [2,4], in this setup a significant ac electric field moves the electrons in the dots with respect to the nuclei. This can be accounted for by introducing a *time-dependent* component in the hyperfine coupling $A_k \to A_k + \tilde{A}_k e^{i\omega t} + \tilde{A}_k^* e^{-i\omega t}$. We estimate that under the present conditions $\tilde{A}_k/A_k \simeq 0.1$ [4,21].

We have considered six candidate mechanisms for DNSP [22], assuming a saturated ESR. We concluded that the dominant one involves the time-dependent hyperfine coupling, which allows for photon assisted flip-flops. These flip-flops do not have a preferred direction set by a large energy mismatch: The spin asymmetry is now provided by internal spin relaxation causing the spin ground state (parallel to the external field) to be more populated than the excited state.

The theoretical consideration includes the following steps: (i) We consider the four (1,1) states using a rotating wave approximation, assuming a saturated ESR and a negligible exchange splitting, i.e. $\min\{t, t^2/\Delta_{LR}\} \ll B_1, B_N$. The eigenstates in a rotating frame are mixtures of spin-up and spin-down states, with a mixing angle $\theta_{L,R} = \frac{1}{2}\arctan\{\tilde{B}_{L,R}/2f_{L,R}\}$ which can be different in both dots (see Fig. 1), due to, e.g., different coupling of the electrons to the CPS. The Rabi frequency in each dot $\tilde{B}_{L,R} \equiv g\mu_B B_1^{(L,R)}/\hbar$ gives the width of the saturated resonance, and the ESR frequency mismatch $f_{L,R} \equiv |g\mu_B(B_0 + B_N^{L,R})/\hbar| - \omega$ depends on the nuclear polarization in each dot. (ii) We evaluate the transition rates between these states to obtain their quasistationary population and the current through the double dot. We include tunneling (characterized by $\Gamma_s = t^2/\Gamma_{\rm out} \simeq$ 1–10 MHz) and single electron spin relaxation [16] ($\propto\Gamma_r \simeq 1$ MHz at zero temperature, which will be enhanced by a thermal factor $k_BT/g\mu_BB_0 \equiv \xi \simeq 5$, in accordance with a lower bound estimate set by the typical leakage current of 100 fA). This approach is valid in the limit $\tilde{B} \gg \Gamma_{s,r}$. (iii) We compute the rates of hyperfine-induced spin exchange. In the first approximation we find rates symmetric with respect to nuclear spin, their scale set by $\Gamma_2 \simeq \tilde{A}_k^2/(64\hbar^2\xi\Gamma_r) \sim$ 0.5 Hz. Being symmetric, these rates do not contribute to DNSP. They merely enhance the relaxation of the nuclear fields. (iv) The small spin-asymmetric part of these rates $\Gamma_1 \simeq \frac{5}{3}(\tilde{A}_k/8\hbar\tilde{B})^2(\Gamma_s/\xi) \sim 10^{-2}$ Hz, due to electron spin relaxation, introduces a preferential direction of nuclear spin pumping in each dot. (v) We construct equations of motion for the effective nuclear fields $B_N^{L,R}$ and analyze the stable states of nuclear polarization given by $dB_N^{L,R}/dt = 0$. (vi) We use a Fokker-Planck equation to give a qualitative analysis of fluctuations of nuclear polarization and switching rates between the stable states.

The evolution equation for B_N^L thus found reads

$$\frac{dB_N^L}{dt} = -\Gamma_1 B_{\rm ov} P(\theta_{L,R}) - \left\{\frac{1}{\tau_n} + \Gamma_2 R(\theta_{L,R})\right\} B_N^L, \qquad (1)$$

and the equation for B_N^R is obtained by permutation of L and R. The field $B_{\rm ov}$ is the Overhauser field of full polarization, $B_{\rm ov} \approx 5$ T for GaAs. The functions P and R are dimensionless functions giving the functional dependence of the resonant nuclear spin pumping (P) and resonantly enhanced nuclear spin relaxation (R) on the mixing angles and on $\Gamma_s/\xi\Gamma_r$, and have a maximum $\sim$1. While R is roughly Lorentzian shaped, the function P is zero far from resonance $\theta \to \{0, \pi\}$, reaches maximum at $|f| \simeq \tilde{B}$, and falls off to zero again at the resonance $\theta = \pi/2$. This resonant dip is due to the vanishing of electron spin polarization at the saturated resonance. In Eq. (1), the terms proportional to $-B_N$ give nuclear spin relaxation: The first term presents the usual τ_n while the second term gives a resonant enhancement owing to spin exchange with electrons. Nuclear spin pumping is given by $\Gamma_1 B_{\rm ov} P$ [$\sim$50 mT/s, much faster than the sweep rate in Fig. 2(a)], with a *sign opposite* to that following from the Overhauser reasoning: Spin exchange under conditions of electron transport is mostly due to electrons polarized along the

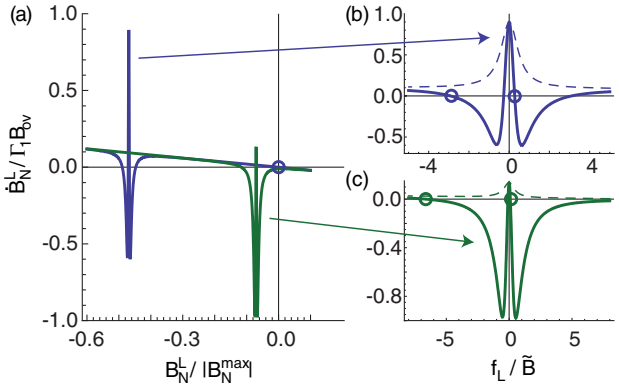

FIG. 3 (color online). (a) Time-derivative dB_N^L/dt at the edge of the hysteresis interval $B_0 \approx B_{\rm res}$ (green) and in the middle of the interval $B_0 \approx B_{\rm res} + 0.5|B_N^{\rm max}|$ (blue). (b),(c) Close-up at resonance. The curves consist of the usual relaxation (linear slope) which is resonantly enhanced (dashed lines), and spin pumping that adds a two-peak shape near the resonance. The circles indicate the stable states of nuclear polarization. We used $\Gamma_1/\Gamma_2 = 0.043$, $\Gamma_2\tau_n = 5$, $\theta_R = 0$, $\xi\Gamma_r/\Gamma_s = 0.75$, and assumed equally strong coupling $\tilde{A}_k$ of all nuclei to the electron.

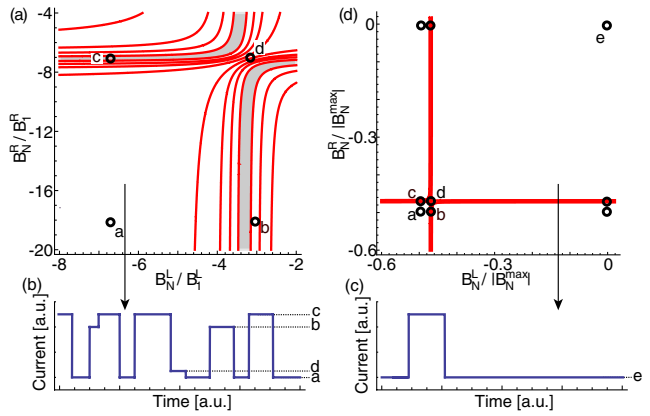

FIG. 4 (color online). Stable polarizations in the plane (B_N^L, B_N^R), for the cases (a) $B_0 - B_{\rm res} \sim B_1$ and (d) $B_0 - B_{\rm res} \sim 0.5|B_N^{\rm max}|$. A contour plot of the current is included, the gray shade indicating the region with highest current. Switching between the stable points gives rise to RTS as presented in (b) and (c). A qualitative difference is that the point e in (d) is ''isolated'', i.e., having switched to e, the system will never switch back. In (a) an asymmetry in $\tilde{B}_{L,R}$ and $N_{L,R}$ is included, resulting in four different current levels for a–d, whereas (d) is plotted assuming a symmetric double dot. Note the different scales at the axes in (a) and (d). The same plots (a) and (d) can be found in the supplementary material [22], where we included the local nuclear spin dynamics as a vector field.

direction of the external field. The shape of a typical pumping curve is shown in Fig. 3.

We are now also able to understand the extended interval of hysteresis: ESR response can be observed as long as there exist stable solutions of $dB_N/dt = 0$ close to resonance. Equation (1) determines the interval of hysteresis as $B_{\rm res} \lesssim B_0 < B_{\rm res} + |B_N^{\rm max}|$, where the maximal nuclear field is $B_N^{\rm max} = -B_{\rm ov}\Gamma_1/(\Gamma_2 + \tau_n^{-1})$. Using the parameters as estimated above we find that $\Gamma_2\tau_n \sim 10$.

The two-peak shape of the pumping curve is responsible for the multiple stable states of nuclear polarization, even at the edge of the hysteresis interval. If $B_0 \approx B_{\rm res}$ (Fig. 3, green curve), there are four stable states for the double dot system. This is represented in Fig. 4(a): The circles indicate the stable points in the plane (B_N^L, B_N^R). It is now clear how, even close to $B_0 = B_{\rm res}$, the system can have *four stable states* with different current. A rough estimate for the duration of the switching between those states is the typical distance ($\sim B_1$) over the local speed of the spin dynamics ($\sim\Gamma_1 B_{\rm ov}$), giving $\sim 10^{-2}$ s, which explains the *fast switching*. A typical time trace in this case will look like Fig. 4(b), which is to be compared with Fig. 2(b).

When increasing B_0, both dots will develop a separate third unpolarized stable state (Fig. 3, blue curve), giving as many as nine stable points, as presented in Fig. 4(d). At higher fields the unpolarized state (labeled e) will become isolated from the other stable states: If the system switches to e, it will never switch back [see Fig. 4(c)]. This also has been observed in experiment [18]. When subsequently sweeping back from high to low field, the barrier for switching back from e to a high-current state is again gradually lowered. When the typical switching time becomes comparable to the time scale of the sweep, the current switches to a high value [Fig. 2(a), lower panel].

From Eq. (1) we construct a Fokker-Planck equation to study the stochastic properties of the polarizations in more detail [16,22]. Importantly, due to the accelerated dynamics, the fluctuations around all polarized states are suppressed as $\langle(\Delta B_N)^2\rangle/\Omega^2 \approx (B_1/|B_N^{\rm max}|)$, $\Omega^2 \equiv (A_k/g\mu_B)^2 N$ being the field variance in the unpolarized state.

To conclude, we have observed multiple nuclear polarization states and locking of the ESR condition over a large range of magnetic fields in a double quantum dot under ESR. We presented a theoretical model that captures the existence of these phenomena and their unusual features as fast switching and a ''wrong'' sign of DNSP.

We acknowledge useful discussions with M. Laforest. This work was supported by the Dutch Foundation for Fundamental Research on Matter (FOM).

[1] R. Hanson *et al.*, Phys. Rev. Lett. **94**, 196802 (2005); M. Atature *et al.*, Science **312**, 551 (2006).
[2] F. H. L. Koppens *et al.*, Nature (London) **442**, 766 (2006).
[3] K. C. Nowack *et al.*, Science **318**, 1430 (2007).
[4] E. A. Laird *et al.*, Phys. Rev. Lett. **99**, 246601 (2007).
[5] M. Kroner *et al.*, Phys. Rev. Lett. **100**, 156803 (2008).
[6] M. Pioro-Ladrière *et al.*, Nature Phys. **4**, 776 (2008).
[7] F. H. L. Koppens *et al.*, Science **309**, 1346 (2005).
[8] J. R. Petta *et al.*, Science **309**, 2180 (2005); A. V. Khaetskii *et al.*, Phys. Rev. Lett. **88**, 186802 (2002).
[9] A. C. Johnson *et al.*, Nature (London) **435**, 925 (2005).
[10] D. Klauser *et al.*, Phys. Rev. B **73**, 205302 (2006).
[11] A. I. Tartakovskii *et al.*, Phys. Rev. Lett. **98**, 026806 (2007).
[12] P. Maletinsky *et al.*, Phys. Rev. Lett. **99**, 056804 (2007).
[13] D. J. Reilly *et al.*, Science **321**, 817 (2008).
[14] V. L. Korenev, Phys. Rev. Lett. **99**, 256405 (2007).
[15] A. W. Overhauser, Phys. Rev. **92**, 411 (1953); A. Abragam, Phys. Rev. **98**, 1729 (1955).
[16] J. Danon and Yu. V. Nazarov, Phys. Rev. Lett. **100**, 056603 (2008).
[17] I. A. Greilich *et al.*, Science **317**, 1896 (2007).
[18] I. T. Vink *et al.*, arXiv:0902.2659.
[19] K. Ono *et al.*, Science **297**, 1313 (2002); A. C. Johnson *et al.*, Phys. Rev. B **72**, 165308 (2005).
[20] D. Paget *et al.*, Phys. Rev. B **15**, 5780 (1977).
[21] M. S. Rudner and L. S. Levitov, Phys. Rev. Lett. **99**, 246602 (2007).
[22] See EPAPS Document No. E-PRLTAO-103-040932 for more theoretical and experimental details. For more information on EPAPS, see http://www.aip.org/pubservs/epaps.html.
[23] Another peak is observed at zero field which manifests the mixing of the four (1, 1) states by the fluctuating nuclear fields [2,7]. An offset of ~7 mT of B_0 due to the superconducting magnet is compensated for in both traces.